Genetic determination of the cellular basis of the sympathetic regulation of bone mass accrual

Daisuke Kajimura,[1] Eiichi Hinoi,[1] Mathieu Ferron,[1] Aruna Kode,[2] Kyle J. Riley,[1] Bin Zhou,[3] X. Edward Guo,[3] and Gerard Karsenty[1]

[1]Department of Genetics and Development and [2]Division of Endocrinology, Department of Medicine, College of Physicians and Surgeons and [3]Bone Bioengineering Laboratory, Department of Biomedical Engineering, Columbia University, New York, NY 10027

The sympathetic nervous system, whose activity is regulated by leptin signaling in the brain, is a major regulator of bone mass accrual. To determine the identity of the cell type in which the sympathetic tone signals to inhibit bone mass accrual, we performed a systematic, cell-specific analysis of the function of the β2 adrenergic receptor (Adrβ2) and various genes implicated in the pathway in the mouse. This was followed by leptin intracerebroventricular (ICV) infusion and bone histomorphometric analyses of bone parameters. We show that the sympathetic tone signals in the osteoblasts to inhibit CREB (cAMP-responsive element-binding protein) phosphorylation and thus decrease osteoblast proliferation and to promote ATF4 phosphorylation and thus increase RANKL (receptor activator of NF-κB ligand) expression, which then stimulates osteoclast differentiation. Leptin ICV infusion in various mouse models established that leptin-dependent inhibition of bone mass accrual relies on both transcriptional events taking place in osteoblasts. Thus, this study formally identifies the osteoblast as the major cell type in which the molecular events triggered by the sympathetic regulation of bone mass accrual take place. As such, it suggests that inhibiting sympathetic signaling could be beneficial in the treatment of low bone mass conditions.

CORRESPONDENCE
Gerard Karsenty:
gk2172@columbia.edu

Abbreviations used: BFR, bone formation rate; CREB, cAMP-responsive element-binding protein; CTx, carboxy-terminal cross-linking telopeptide of type I collagen; ICV, intracerebroventricular.

A notable recent advance in our understanding of the genetic and molecular control of bone remodeling has been uncovering the influence exerted on this process by the brain, a process generally referred to as the central control of bone mass (Karsenty, 2006). This complex, multistep process starts with the secretion of serotonin by brainstem neurons that then binds to a specific receptor in neurons of the ventromedial nuclei of the hypothalamus (Yadav et al., 2009). Serotonergic signaling in these neurons leads to a decrease in the activity of the sympathetic nervous system, which normally acts on osteoblasts to decrease bone formation and to increase osteoclast differentiation and bone resorption (Takeda et al., 2002; Elefteriou et al., 2004, 2005; Fu et al., 2005).

Remarkably, and adding further complexity to the central control of bone mass, this entire regulatory loop has been shown to be under the control of the adipocyte-derived hormone leptin, which inhibits bone mass accrual by hampering synthesis and secretion of serotonin by brainstem neurons (Ducy et al., 2000; Yadav et al., 2009). Indeed, a cell-specific gene inactivation approach showed that a deletion of the leptin receptor in osteoblasts only does not affect bone mass accrual, whereas the same deletion in neurons recapitulates the bone phenotype observed in *ob/ob* mice (Shi et al., 2008). These data demonstrate that the bulk of leptin regulation of bone mass accrual occurs through a neuronal relay, which was identified as being the sympathetic tone (Takeda et al., 2002).

Previous studies have established that the sympathetic tone lowers bone mass accrual by acting through the β2 adrenergic receptor. These studies also identified CREB (cAMP-responsive element-binding protein) and cMyc as mediators of the sympathetic inhibition of proliferation and ATF4 as a mediator of its regulation of osteoclast differentiation (Elefteriou et al., 2005; Fu et al., 2005). Remarkably however,

The Rockefeller University Press $30.00
J. Exp. Med. Vol. 208 No. 4 841-851
www.jem.org/cgi/doi/10.1084/jem.20102608

The Journal of Experimental Medicine

until now, the identity of the cell in which the sympathetic tone acts to inhibit bone mass accrual has remained elusive. The reason for this ambiguity is that no cell-specific gene deletion of the β2 adrenergic receptor (*Adrβ2*) experiments have been reported yet (Elefteriou et al., 2005; Fu et al., 2005). This is obviously an important question, as the nature of the sympathetic target cells ultimately defines how leptin regulates bone mass accrual.

To address this important lingering issue regarding the peripheral mediation of the central control of bone mass, we have embarked on a systematic, cell-specific analysis of the aforementioned key molecular players. This analysis demonstrates that *Adrβ2*, *Creb*, and *cMyc* and *Atf4* act in osteoblasts to control osteoblast proliferation and osteoclast differentiation, respectively, and that this pathway is influenced by leptin. As such, this study provides a more complete understanding of the central control of bone mass and opens a new therapeutic avenue for low bone mass diseases.

RESULTS

Adrβ2 regulates bone mass accrual through its expression in osteoblasts

To identify the cell type in which the sympathetic nervous system acts to regulate bone mass accrual, we relied on cell-specific gene inactivation in the mouse. To determine whether the sympathetic tone signals in osteoblasts to regulate bone mass accrual, we generated a mutant mouse strain expressing a floxed allele of *Adrβ2*, the adrenergic receptor whose deletion in all cells affects bone mass accrual (Elefteriou et al., 2005). These mutant mice were crossed with α*1(I) Collagen* (2.3-kb *Col1a1* promoter)–*Cre* transgenic mice to delete the gene in osteoblasts only ($Adr\beta2_{osb}^{-/-}$ mice; Dacquin et al., 2002). Before analyzing the mutant mice, we verified that we had achieved a high percentage of recombination at the *Adrβ2* locus in osteoblasts but in no other cell types (Fig. 1, A and B).

As it is the case in mice lacking *Adrβ2* in all cells (Elefteriou et al., 2005), $Adr\beta2_{osb}^{-/-}$ mice had a normal bone mass until 12 wk of age (Fig. 1 L). However, at 24 wk of age, $Adr\beta2_{osb}^{-/-}$ mice presented a distinct high bone mass phenotype affecting both vertebrates and long bones (Fig. 1, C and D), whose severity was similar to the one observed in mice lacking *Adrβ2* in all cells. Histomorphometric analysis of vertebrae showed that this high bone mass phenotype was caused by a concomitant increase in the number of osteoblasts and bone formation rate (BFR) and a decrease in the osteoclast number (Fig. 1 C). As expected, the decrease in osteoclast number did result in a decrease in bone resorption activity, as determined by serum levels of carboxy-terminal cross-linking telopeptide of type I collagen (CTx), which was decreased in $Adr\beta2^{-/-}$ mice (Fig. 1 H). These results established that the osteoblast is a major target of the sympathetic tone regulation of bone mass accrual.

Our previously published work (Fu et al., 2005) has established that the sympathetic tone in osteoblasts regulates phosphorylation of CREB on serine 133 and of ATF4 on serine 254. Moreover, these two events should be altered by leptin signaling in the brain, whose function is to decrease bone formation by increasing sympathetic tone (Takeda et al., 2002). In full agreement with this model, leptin intracerebroventricular (ICV) infusion decreased CREB phosphorylation in control but not in $Adr\beta2_{osb}^{-/-}$ bones (Fig. 1 E). These observations indicated that the sympathetic signaling in osteoblasts is downstream of leptin signaling in the brain.

At the molecular level, we observed that expression of *CyclinD1*, *CyclinD2*, *CyclinE1*, *cMyc*, and *Per1*, all genes implicated in the sympathetic regulation of bone mass accrual (Fu et al., 2005), was significantly increased in $Adr\beta2_{osb}^{-/-}$ bones (Fig. 1 F). Similarly, the expression of *Cry1* and *Cry2* was increased (Fig. S2 A). In contrast, the ratio of *Rankl* to *Opg* expression was decreased (Fig. 1 G). Based on these results, we anticipated that leptin ICV infusion, a procedure which decreases bone mass by decreasing bone formation parameters and increasing bone resorption parameters in WT mice, should fail to do so in $Adr\beta2_{osb}^{-/-}$ mice. That is exactly what was observed in 12-wk-old $Adr\beta2_{osb}^{-/-}$ mice (Fig. 1, I–M). In summary, the analysis of mice lacking *Adrβ2* only in osteoblasts established that the sympathetic tone lowers bone mass accrual by signaling in osteoblasts through the Adrβ2. The clarity of the effect (and lack) of leptin ICV infusion in WT (and $Adr\beta2_{osb}^{-/-}$ mice) led us to use this assay as a tool to verify in the rest of the study the cell-specific nature of other aspects of the leptin/sympathetic regulation of bone mass accrual.

Leptin inhibition of bone mass accrual requires *Creb* expression in osteoblasts

Previous experiments have suggested that the sympathetic tone acts, in osteoblasts, through CREB to regulate bone formation and that leptin signaling in the brain affects this process (Fu et al., 2005). To determine whether it is indeed the case, we generated, using the aforementioned strategy, mice lacking CREB in osteoblasts only ($Creb_{osb}^{-/-}$ mice) and, as we did in all experiments, verified that we had achieved an efficient and cell-specific gene deletion before using these mutant mice (Fig. 2, A and B).

CREB has recently emerged as a more important than anticipated positive transcriptional regulator of bone formation (Yadav et al., 2008, 2009; Datta and Abou-Samra, 2009; Oury et al., 2010). In particular, it has been shown to be a transcriptional effector of the anabolic action of parathyroid hormone (Datta and Abou-Samra, 2009), while its function is inhibited by gut-derived serotonin, which is a negative regulator of bone formation (Yadav et al., 2008). Given the existence of these two important regulations, it is no surprise that at 12 wk of age, $Creb_{osb}^{-/-}$ mice display low bone mass because of an isolated decrease in bone formation parameters (Fig. 2 C). Nevertheless, to determine whether CREB is a transcriptional mediator of the sympathetic tone-dependent regulation of bone formation, we studied the expression of genes regulated by the sympathetic tone in $Creb_{osb}^{-/-}$ bones. As was the case in $Adr\beta2_{osb}^{-/-}$ bones, expression of genes implicated in the sympathetic regulation of bone formation,

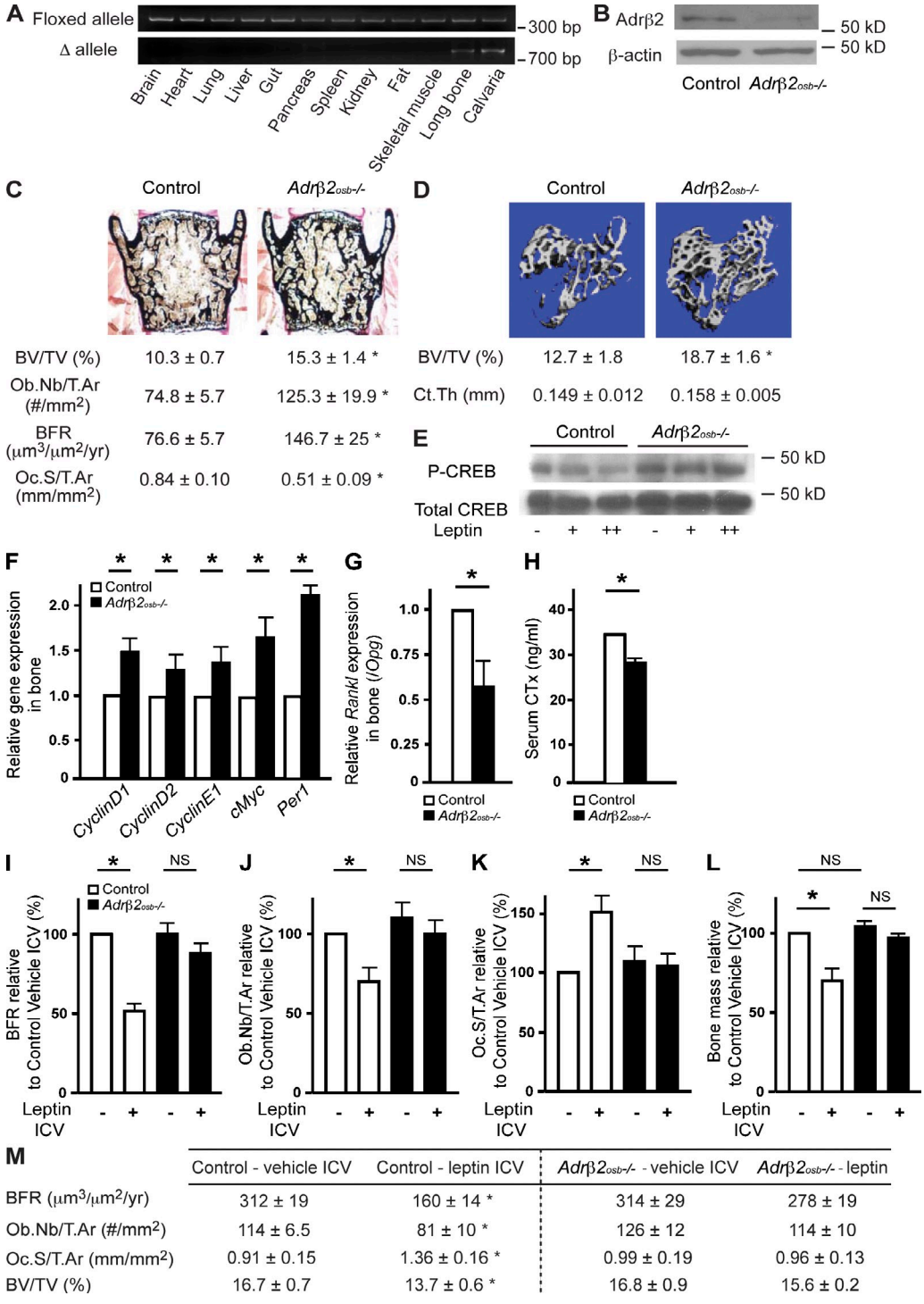

Figure 1. Analysis of *Adrβ2*$_{osb}^{-/-}$ mice. (A) Specificity of α *1(I) Collagen–Cre*-driven deletion of *Adrβ2* allele in bone. (B) Expression level of Adrβ2 protein in bone marrow–derived osteoblasts. (C) Bone histomorphometric analysis *Adrβ2*$_{osb}^{-/-}$ mice at 24 wk of age (control, $n = 11$; *Adrβ2*$_{osb}^{-/-}$, $n = 7$). Mineralized bone matrix is stained in black by Von Kossa reagent. Histomorphometric parameters: BV/TV, bone volume over tissue volume; Ob.Nb/T.Ar, number of osteoblasts per trabecular area; Oc.S/T.Ar, osteoclast surface per trabecular area. (D) μCT analysis of control ($n = 6$) and *Adrβ2*$_{osb}^{-/-}$ ($n = 5$) proximal tibiae at 24 wk of age. Ct.Th, cortical thickness. (E) Expression of phospho-CREB and total CREB after 28-d leptin ICV infusion at 12 wk of age. (F and G) Expression of various genes in control ($n = 7$) and *Adrβ2*$_{osb}^{-/-}$ ($n = 7$) bone at 24 wk of age. (H) Serum CTx levels of control ($n = 8$) and *Adrβ2*$_{osb}^{-/-}$ ($n = 7$) mice at 24 wk of age. (I–L) Bone histomorphometric analysis of 12-wk-old *Adrβ2*$_{osb}^{-/-}$ mice after leptin ICV infusion shown as percentage compared with control mice treated with vehicle ICV infusion (control mice with vehicle ICV infusion, $n = 9$; control mice with leptin ICV infusion, $n = 8$; *Adrβ2*$_{osb}^{-/-}$ mice with vehicle ICV infusion, $n = 5$; *Adrβ2*$_{osb}^{-/-}$ mice with leptin ICV infusion, $n = 5$). (M) Bone histomorphometric analysis of 12-wk-old *Adrβ2*$_{osb}^{-/-}$ mice after leptin ICV infusion. All experiments were performed independently at least twice, and representative data are shown. Results are shown as mean ± SEM. Statistical analysis was performed by Student's *t* test. For all panels: *, $P < 0.05$.

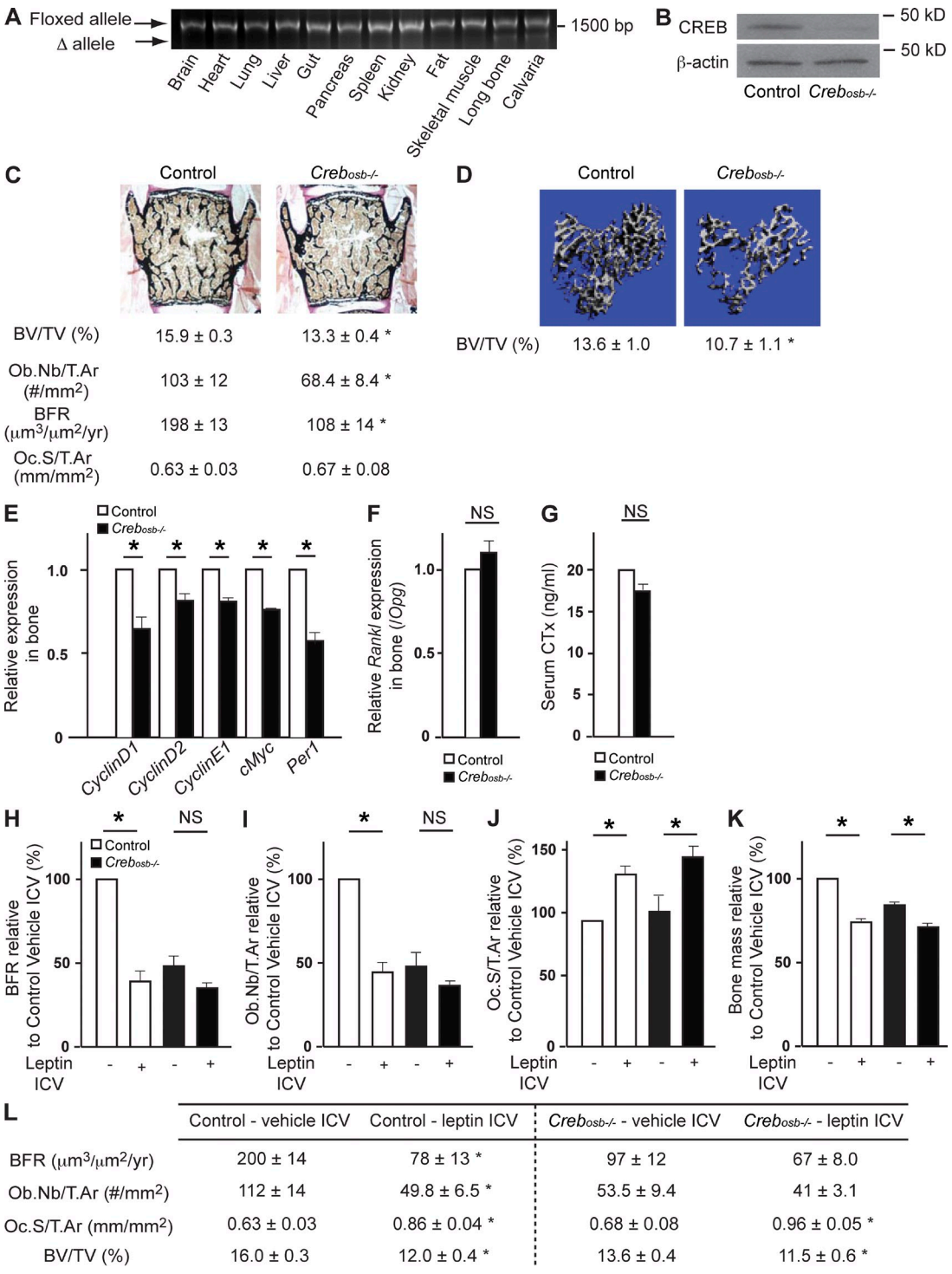

Figure 2. Analysis of *Creb*$_{osb}^{-/-}$ mice. (A) Specificity of α*1(I) Collagen–Cre*-driven deletion of *Creb* allele in bone. (B) Expression level of the CREB protein in bone marrow–derived osteoblasts. (C) Bone histomorphometric analysis of *Creb*$_{osb}^{-/-}$ mice at 12 wk of age (control, $n = 14$; *Creb*$_{osb}^{-/-}$, $n = 12$). BV/TV, bone volume over tissue volume; Ob.Nb/T.Ar, number of osteoblasts per trabecular area; Oc.S/T.Ar, osteoclast surface per trabecular area. (D) μCT analysis of control ($n = 5$) and *Creb*$_{osb}^{-/-}$ ($n = 5$) proximal tibiae at 12 wk of age. (E and F) Expression of various genes in control ($n = 7$) and *Creb*$_{osb}^{-/-}$ ($n = 3$) bone at 12 wk of age. (G) Serum CTx levels of control ($n = 7$) and *Creb*$_{osb}^{-/-}$ ($n = 7$) mice at 12 wk of age. (H–K) Bone histomorphometric analysis of *Creb*$_{osb}^{-/-}$ mice after leptin ICV infusion at 12 wk of age shown as percentage compared with control mice with vehicle ICV infusion (control mice with vehicle ICV infusion, $n = 14$; control mice with leptin ICV infusion, $n = 12$; *Creb*$_{osb}^{-/-}$ mice with vehicle ICV infusion, $n = 8$; *Creb*$_{osb}^{-/-}$ mice with leptin ICV infusion, $n = 10$). (L) Bone histomorphometric analysis of 12-wk-old *Creb*$_{osb}^{-/-}$ mice after leptin ICV infusion. All experiments were performed independently at least twice, and representative data are shown. Results are shown as mean ± SEM. Statistical analysis was performed by Student's *t* test. For all panels: *, $P < 0.05$.

CyclinD1, *CyclinD2*, *CyclinE1*, *Per1*, and *cMyc*, was affected in $Creb_{osb}^{-/-}$ bones (Fig. 2 E). Consistent with the decreased expression of cell cycle regulator genes, osteoblast proliferation, as measured by BrdU incorporation, was markedly reduced in $Creb_{osb}^{-/-}$ bones (Fig. S2 B). In contrast, the ratio of *Rankl* to *Opg* expression and bone resorption measured by serum CTx levels were not affected (Fig. 2, F and G). Thus, CREB, through its expression in osteoblasts, regulates osteoblast proliferation.

Next, we asked whether leptin signaling ultimately requires *Creb* expression in osteoblasts to inhibit bone mass accrual. As shown in Fig. 2 (H, I, and L), long-term leptin ICV infusion failed to decrease bone formation parameters, although it could increase osteoclast number in $Creb_{osb}^{-/-}$ mice (Fig. 2, J and L). As a result, leptin ICV infusion decreased, albeit mildly, bone volume in $Creb_{osb}^{-/-}$ mice (Fig. 2, K and L).

The fact that leptin ICV infusion could decrease bone volume in $Creb_{osb}^{-/-}$ mice can be explained only if one hypothesizes that the sympathetic tone can increase bone resorption independently from CREB, possibly through ATF4. If it is the case, one would expect that by deleting *Creb* in osteoblasts, one would blunt the inhibition of bone formation induced by the sympathetic tone, without affecting bone resorption.

Leptin regulation of bone resorption requires *Atf4* expression in osteoblasts

If the aforementioned explanation of the bone phenotype of $Creb_{osb}^{-/-}$ mice and of the influence that leptin exerts on it is correct, it could be verified through the use of mice lacking *Atf4* in osteoblasts only (Fig. 3). As is the case in mice lacking *Atf4* in all cells, $Atf4_{osb}^{-/-}$ mice have a low bone mass phenotype caused by a decrease in bone formation parameters (Fig. 3 C; Yang et al., 2004; Elefteriou et al., 2006). The decrease in bone formation parameters could be explained, at least in part, by an alteration in osteoblast differentiation because expression of two ATF4 target genes, *Bglap1* and *Col1a1*, was significantly reduced in $Atf4_{osb}^{-/-}$ bone (Fig. S2 C). On the contrary, unlike what is the case in $Adr\beta2_{osb}^{-/-}$ and $Creb_{osb}^{-/-}$ mice, expression of cell cycle regulator genes *CyclinD1*, *CyclinD2*, *CyclinE1*, *Per1*, and *cMyc* was not affected (Fig. 3 E). These results are consistent with the hypothesis that the expression of these genes in osteoblasts is under the control of CREB, not ATF4 (Fig. 2; Fu et al., 2005). In contrast, the ratio of *Rankl* to *Opg* expression was lower in $Atf4_{osb}^{-/-}$ mice (Fig. 3 F). To formally verify our hypothesis, we then infused leptin ICV in control and $Atf4_{osb}^{-/-}$ mice. Leptin ICV infusion increased the osteoclast number in control but not in $Atf4_{osb}^{-/-}$ mice (Fig. 3, J and L). However, this procedure decreased bone formation in both control and mutant mice. This was expected because CREB signaling is intact in $Atf4_{osb}^{-/-}$ bones. That leptin ICV infusion could decrease bone formation parameters (Fig. 3, H, I, and L) explains also why it could decrease bone mass on $Atf4_{osb}^{-/-}$ mice (Fig. 3, K and L).

Collectively, the analysis of cell-specific gene inactivation mouse models for two distinct transcription factors presented in Figs. 2 and 3 suggested a model whereby the sympathetic tone uses CREB and ATF4 in osteoblasts to influence bone formation and bone resorption, respectively (Fig. S1).

Leptin inhibition of bone mass accrual requires *cMyc* expression in osteoblasts

We have shown earlier that downstream of the sympathetic regulation of bone formation, *cMyc* must be a target of CREB (Fu et al., 2005). To determine whether *cMyc* carries out this function through its expression in osteoblasts, we used the same strategy used for the study of *Adrβ2* and *Creb* and *Atf4* functions in osteoblasts (Figs. 1–3) and again verified before using them that we had achieved an efficient and osteoblast-specific deletion in $cMyc_{osb}^{-/-}$ mice (Fig. 4, A and B).

We should emphasize here that unlike other mutant mice, $cMyc_{osb}^{-/-}$ mice were maintained on a mixed genetic background including C57/B6 and 129Sv/EV. This difference in genetic background explains the rather high bone volume observed in control *cMyc-flox/flox* and mutant $cMyc_{osb}^{-/-}$ littermates compared with other mutant mice that were all on a pure C57/B6 background (Fig. 4 C). Notwithstanding this feature, and when compared with *cMyc-flox/flox* mice, $cMyc_{osb}^{-/-}$ mice demonstrated a low bone mass phenotype at 12 wk of age that was secondary to a decrease in bone formation parameters (Fig. 4 C). The osteoclast number and activity were not significantly affected in $cMyc_{osb}^{-/-}$ mice (Fig. 4, C and G). Consistent with the notion that *cMyc* may be a target gene of the sympathetic tone and CREB in osteoblasts, expression of the cyclin genes *CyclinD1*, *CyclinD2*, and *CyclinE1* was also significantly decreased in $cMyc_{osb}^{-/-}$ bones (Fig. 4 E). In contrast, the expression ratio of *Rankl* to *Opg* was not affected (Fig. 4 F). The expression of *Opg* was not affected in $cMyc_{osb}^{-/-}$ bones (Fig. S3, A–D).

To determine formally that leptin inhibition of bone mass accrual requires the expression of *cMyc* in osteoblasts, we performed long-term leptin ICV infusion in control and $cMyc_{osb}^{-/-}$ mice. As shown in Fig. 4 (H, I, and L), leptin ICV infusion decreased bone formation parameters in control but not in $cMyc_{osb}^{-/-}$ mice. In contrast, and in full agreement with the ATF4 mediation of this aspect of the regulation of bone mass accrual, leptin ICV infusion increased bone resorption parameters equally well in control and in $cMyc_{osb}^{-/-}$ mice (Fig. 4, J and L). As a result, leptin decreased bone mass in both control and in $cMyc_{osb}^{-/-}$ mice, although the effect was more pronounced in control mice (Fig. 4, K and L).

Genetic interaction between *Adrβ2*, *Creb*, and *cMyc* expression in osteoblasts downstream of leptin signaling

In the last part of these experiments, we sought to establish that the leptin regulation of bone mass accrual requires the various transcription factors studied in this paper to interact in the osteoblasts. This is a particularly important aspect of our work because CREB, for instance, can be activated by a protein kinase A–dependent but also by other, unrelated pathways.

Consistent with the notion that *cMyc* is a downstream target gene of CREB, $cMyc_{osb}^{-/-}$ mice showed a similar phenotype as $Creb_{osb}^{-/-}$ mice as well as a similar response to long-term

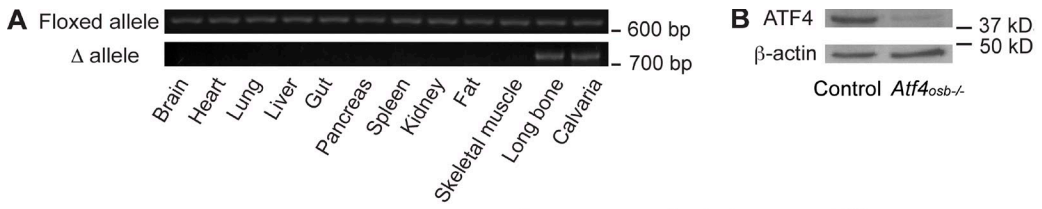

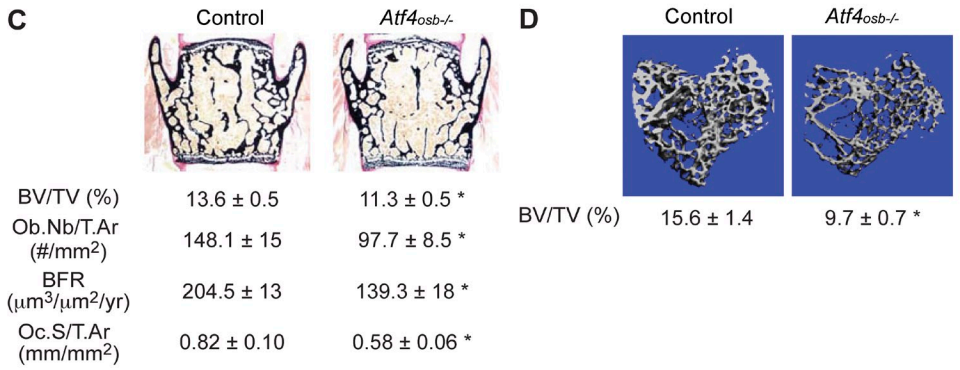

	Control	*Atf4*$_{osb-/-}$
BV/TV (%)	13.6 ± 0.5	11.3 ± 0.5 *
Ob.Nb/T.Ar (#/mm^2)	148.1 ± 15	97.7 ± 8.5 *
BFR (μm^3/μm^2/yr)	204.5 ± 13	139.3 ± 18 *
Oc.S/T.Ar (mm/mm^2)	0.82 ± 0.10	0.58 ± 0.06 *

	Control	*Atf4*$_{osb-/-}$
BV/TV (%)	15.6 ± 1.4	9.7 ± 0.7 *

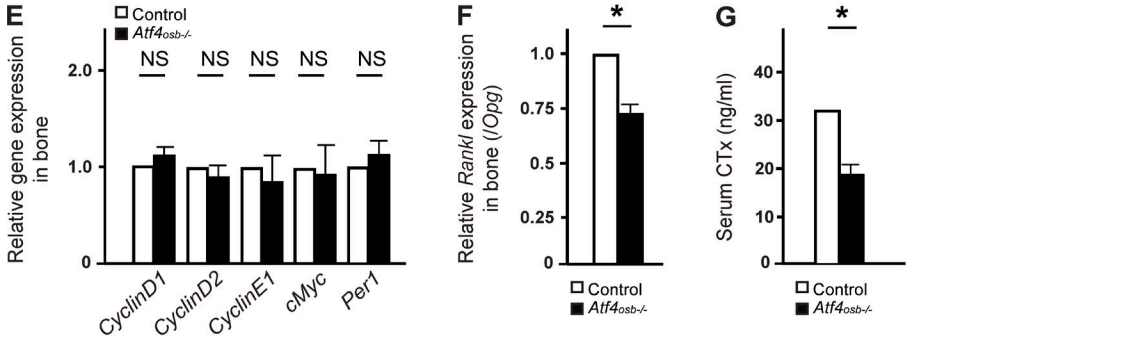

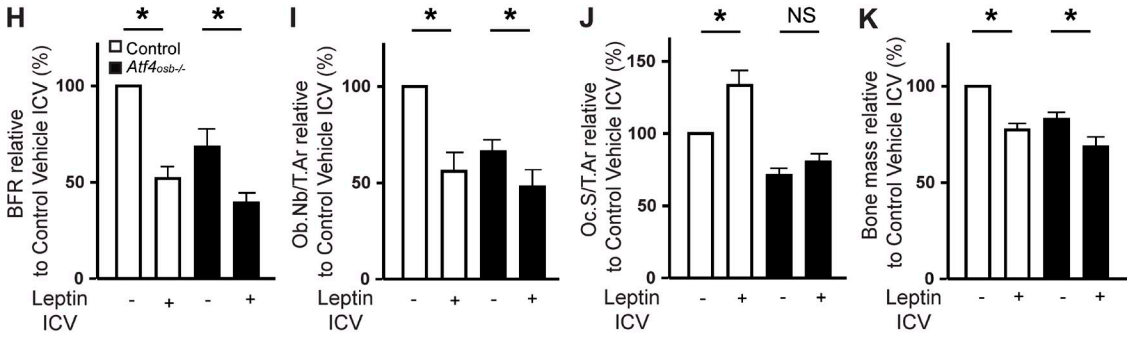

L

	Control - vehicle ICV	Control - leptin ICV	*Atf4*$_{osb-/-}$ - vehicle ICV	*Atf4*$_{osb-/-}$ - leptin
BFR (μm^3/μm^2/yr)	205 ± 13	106 ± 13 *	139 ± 18	80 ± 8.1 *
Ob.Nb/T.Ar (#/mm^2)	148 ± 15	84 ± 15 *	98 ± 8.5	71 ± 11 *
Oc.S/T.Ar (mm/mm^2)	0.82 ± 0.1	1.10 ± 0.16 *	0.58 ± 0.06	0.66 ± 0.09
BV/TV (%)	13.6 ± 0.5	10.5 ± 0.4 *	11.3 ± 0.5	9.3 ± 0.7 *

Figure 3. Analysis of *Atf4*$_{osb}^{-/-}$ mice. (A) Specificity of α*1(I) Collagen–Cre*-driven deletion of *Atf4* allele in bone. (B) Expression level of the ATF4 protein in bone. (C) Bone histomorphometric analysis of *Atf4*$_{osb}^{-/-}$ mice at 12 wk of age (control, $n = 10$; *Atf4*$_{osb}^{-/-}$, $n = 9$). BV/TV, bone volume over tissue volume; Ob.Nb/T.Ar, number of osteoblasts per trabecular area; Oc.S/T.Ar, osteoclast surface per trabecular area. (D) μCT analysis of control ($n = 5$) and *Atf4*$_{osb}^{-/-}$ ($n = 5$) proximal tibiae at 12 wk of age. (E and F) Expression of various genes in control ($n = 9$) and *Atf4*$_{osb}^{-/-}$ ($n = 9$) bone at 12 wk of age. (G) Serum CTx levels of control ($n = 8$) and *Atf4*$_{osb}^{-/-}$ mice ($n = 8$) at 12 wk of age. (H–K) Bone histomorphometric analysis of *Atf4*$_{osb}^{-/-}$ mice after leptin ICV infusion at 12 wk of age shown as percentage compared with control mice treated with vehicle ICV infusion (control mice with vehicle ICV infusion, $n = 10$; control mice with leptin ICV infusion, $n = 9$; *Atf4*$_{osb}^{-/-}$ mice with vehicle ICV infusion, $n = 9$; *Atf4*$_{osb}^{-/-}$ mice with leptin ICV infusion, $n = 9$). (L) Bone histomorphometric analysis of 12-wk-old *Atf4*$_{osb}^{-/-}$ mice after leptin ICV infusion. All experiments were performed independently at least twice, and representative data are shown. Results are shown as mean ± SEM. Statistical analysis was performed by Student's *t* test. For all panels: *, $P < 0.05$.

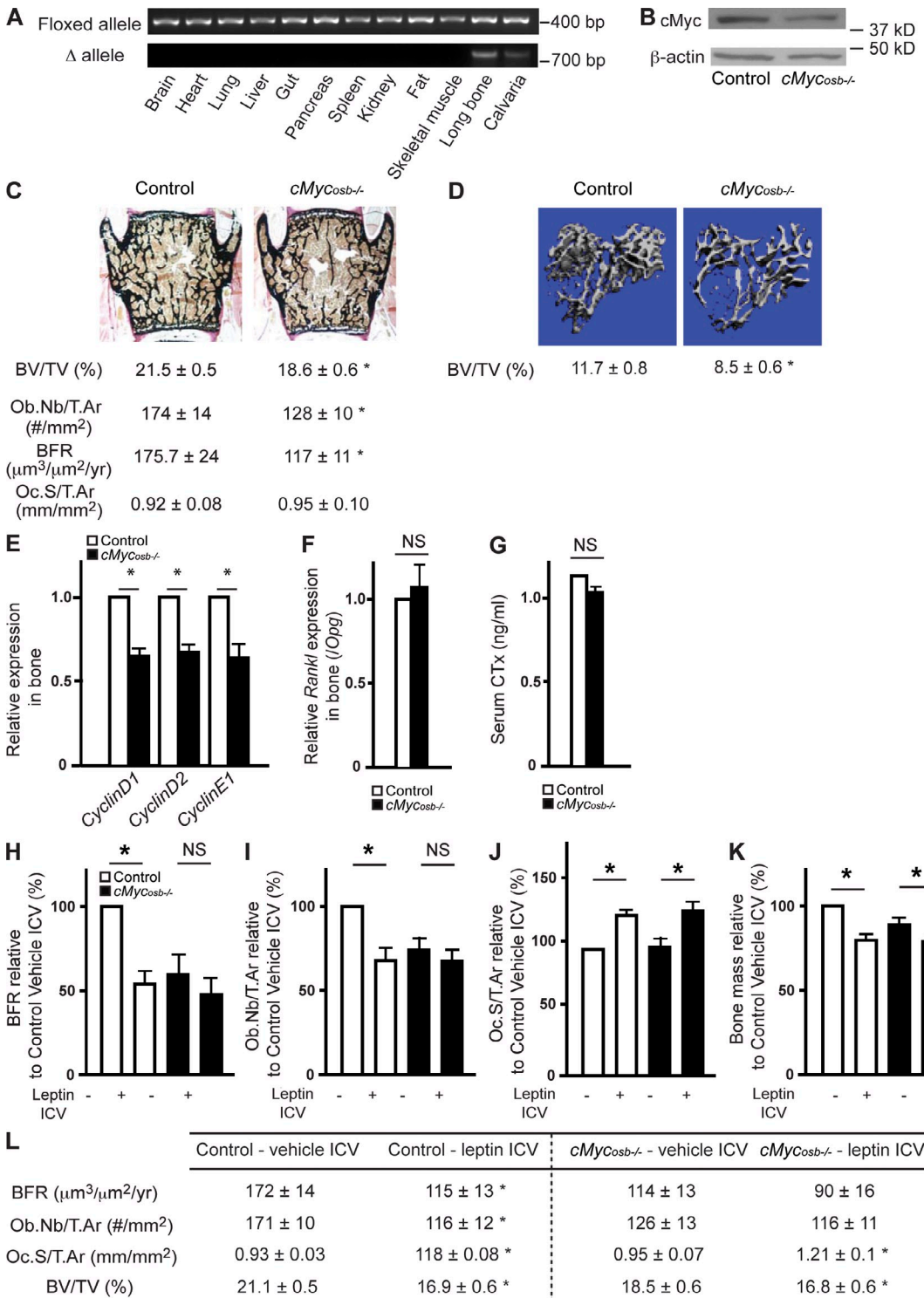

L

	Control - vehicle ICV	Control - leptin ICV	*cMyc*$_{osb}^{-/-}$ - vehicle ICV	*cMyc*$_{osb}^{-/-}$ - leptin ICV
BFR (μm³/μm²/yr)	172 ± 14	115 ± 13 *	114 ± 13	90 ± 16
Ob.Nb/T.Ar (#/mm²)	171 ± 10	116 ± 12 *	126 ± 13	116 ± 11
Oc.S/T.Ar (mm/mm²)	0.93 ± 0.03	118 ± 0.08 *	0.95 ± 0.07	1.21 ± 0.1 *
BV/TV (%)	21.1 ± 0.5	16.9 ± 0.6 *	18.5 ± 0.6	16.8 ± 0.6 *

Figure 4. Analysis of *cMyc*$_{osb}^{-/-}$ mice. (A) Specificity of α *1(I) Collagen–Cre*-driven deletion of *cMyc* allele in bone. (B) Expression level of the cMyc protein in bone marrow–derived osteoblasts. (C) Bone histomorphometric analysis of *cMyc*$_{osb}^{-/-}$ mice at 12 wk of age (control, $n = 14$; *cMyc*$_{osb}^{-/-}$, $n = 9$). BV/TV, bone volume over tissue volume; Ob.Nb/T.Ar, number of osteoblasts per trabecular area; Oc.S/T.Ar, osteoclast surface per trabecular area. (D) μCT analysis of control ($n = 5$) and *cMyc*$_{osb}^{-/-}$ ($n = 5$) proximal tibiae at 12 wk of age. (E and F) Expression of various genes in control ($n = 3$) and *cMyc*$_{osb}^{-/-}$ ($n = 7$) bone at 12 wk of age. (G) Serum CTx levels of control ($n = 6$) and *cMyc*$_{osb}^{-/-}$ ($n = 6$) at 12 wk of age. (H–K) Bone histomorphometric analysis of *cMyc*$_{osb}^{-/-}$ mice after leptin ICV infusion at 12 wk of age shown as percentage compared with control mice treated with vehicle ICV infusion (control mice with vehicle ICV infusion, $n = 14$; control mice with leptin ICV infusion, $n = 8$; *cMyc*$_{osb}^{-/-}$ mice with vehicle ICV infusion, $n = 9$; *cMyc*$_{osb}^{-/-}$ mice with leptin ICV infusion, $n = 10$). (L) Bone histomorphometric analysis of 12-wk-old *cMyc*$_{osb}^{-/-}$ mice after leptin ICV infusion. All experiments were performed independently at least twice, and representative data are shown. Results are shown as mean ± SEM. Statistical analysis was performed by Student's *t* test. For all panels: *, $P < 0.05$.

leptin ICV infusion. To verify in vivo that these genes are in the same pathway downstream of leptin signaling in osteoblasts, we generated $Creb_{osb}^{+/-}$;$cMyc_{osb}^{+/-}$ compound heterozygous mice. That $Creb_{osb}^{+/-}$;$cMyc_{osb}^{+/-}$ mice had decreased bone formation parameters, while bone resorption parameters were not affected (Fig. 5, A–E), supports the notion that both *Creb* and *cMyc* regulate osteoblast proliferation in osteoblasts but not osteoclast differentiation.

Next, we asked whether the high bone mass phenotype of the $Adr\beta2_{osb}^{-/-}$ mice could be corrected by removing one copy of *cMyc* in osteoblasts. As shown in Fig. 5 (F–J) and Fig. S4, removing one allele of *cMyc* in osteoblasts normalized bone formation parameters in $Adr\beta2_{osb}^{-/-}$ mice. In contrast, this manipulation did not affect the bone resorption parameters in $Adr\beta2_{osb}^{-/-}$ mice, further indicating that the sympathetic tone uses different transcriptional mediators to regulate bone formation and bone resorption. Thus, the analysis of these compound mutant mouse strains verified the existence of an interaction between *Adrβ2*, *Creb*, and *cMyc* in the osteoblast to allow the sympathetic nervous system to prevent bone mass accrual.

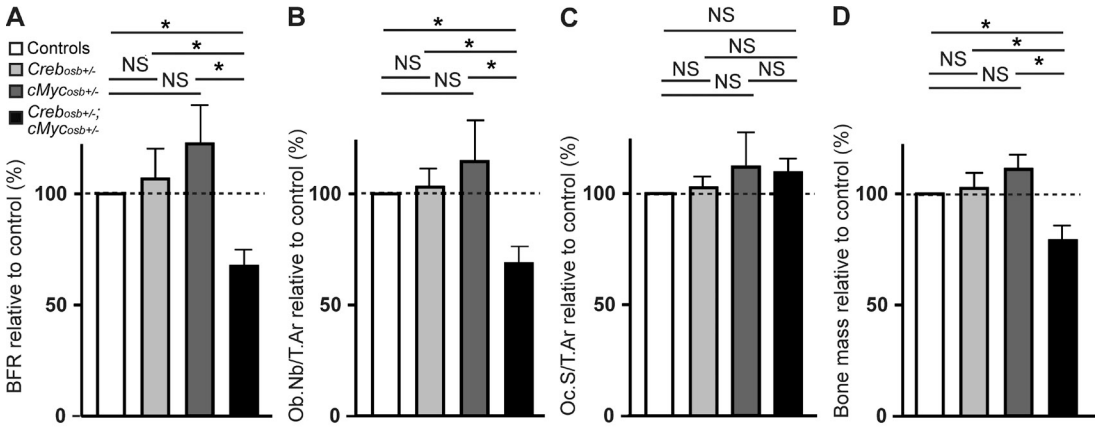

E

	Controls	*Creb*$_{osb+/-}$	*cMyc*$_{osb+/-}$	*Creb*$_{osb+/-}$;*cMyc*$_{osb+/-}$
BFR (μm³/μm²/yr)	147 ± 15	156 ± 20	178 ± 24	109 ± 10 *
Ob.Nb/T.Ar (#/mm²)	156 ± 17	160 ± 13	178 ± 35	106 ± 10 *
Oc.S/T.Ar (mm/mm²)	0.70 ± 0.07	0.70 ± 0.06	0.78 ± 0.2	0.77 ± 0.09
BV/TV (%)	14.8 ± 0.6	15.2 ± 0.9	16.5 ± 0.9	11.7 ± 0.9 *

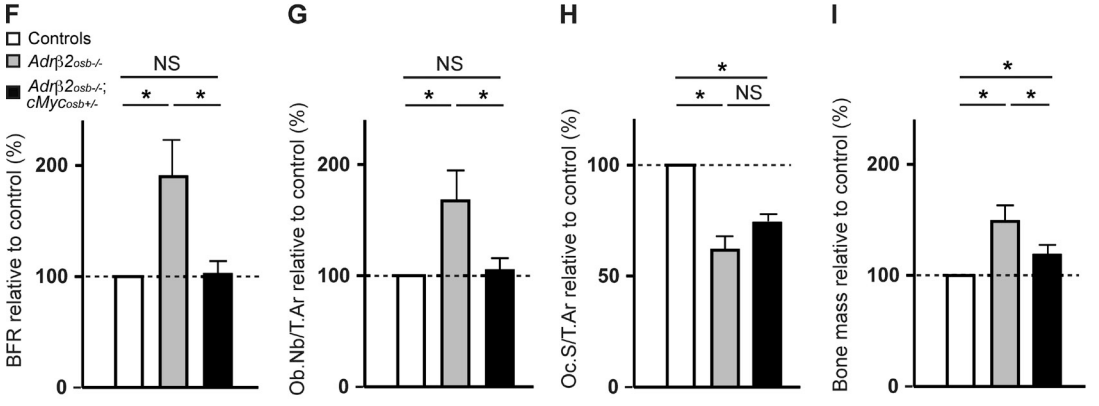

J

	Controls	*Adrβ2*$_{osb-/-}$	*Adrβ2*$_{osb-/-}$;*cMyc*$_{osb+/-}$
BFR (μm³/μm²/yr)	77 ± 5.7	147 ± 25 *	78 ± 8.8
Ob.Nb/T.Ar (#/mm²)	75 ± 4.5	125 ± 20 *	78 ± 7.8
Oc.S/T.Ar (mm/mm²)	0.84 ± 0.1	0.51 ± 0.09 *	0.62 ± 0.05 *
BV/TV (%)	10.3 ± 0.7	15.3 ± 1.4 *	12.2 ± 0.7 *,**

Figure 5. Genetic epistasis analysis. (A–E) Bone histomorphometric analysis of $Creb_{osb}^{+/-}$;$cMyc_{osb}^{+/-}$ mice at 12 wk of age (controls, $n = 15$; $Creb_{osb}^{+/-}$, $n = 9$; $cMyc_{osb}^{+/-}$, $n = 4$; $Creb_{osb}^{+/-}$;$cMyc_{osb}^{+/-}$, $n = 8$). (F–J) Bone histomorphometric analysis of $Adr\beta2_{osb}^{-/-}$;$cMyc_{osb}^{+/-}$ mice at 24 wk of age (controls, $n = 11$; $Adr\beta2_{osb}^{-/-}$, $n = 7$; $Adr\beta2_{osb}^{-/-}$;$cMyc_{osb}^{+/-}$, $n = 9$). *, $P < 0.05$ between controls; **, $P < 0.05$ between $Adr\beta2_{osb}^{-/-}$ mice and $Adr\beta2_{osb}^{-/-}$;$cMyc_{osb}^{+/-}$ mice. Experiments were performed independently twice, and representative data are shown. Results are shown as mean ± SEM. Dashed lines indicate control value of 100%. BV/TV, bone volume over tissue volume; Ob.Nb/T.Ar, number of osteoblasts per trabecular area; Oc.S/T.Ar, osteoclast surface per trabecular area.

DISCUSSION

In this study, we used genetic and pharmacological means to formally identify the osteoblast as the major cell type in which the sympathetic tone, under the control of leptin signaling in the brain, acts to inhibit bone mass accrual. Results of this investigation are represented schematically in Fig. S1. We cannot exclude, based on our results, the possibility that osteocytes may also be a target of the sympathetic tone. We should emphasize here that our study is restricted to the means whereby leptin signaling in the brain, as represented by leptin ICV infusion, regulates bone mass. The reason for this focus on this aspect of leptin regulation of bone mass accrual is that a neuron-specific inactivation of the leptin receptor in the mouse recapitulates the bone phenotype of mice lacking leptin signaling, whereas its osteoblast-specific inactivation fails to do so (Shi et al., 2008).

Once it was realized that there was a central control of bone mass (Ducy et al., 2000), the next question was to decipher how the brain signals to the bone. It became rapidly apparent that the sympathetic nervous system is a critical mediator of this homeostatic function exerted by the brain. This signaling inhibits bone mass accrual by, at the same time, preventing bone formation and favoring bone resorption. The evidence supporting this view was genetic and relied on the study of a classical gene inactivation mouse model. Indeed, mice lacking the β2 adrenergic receptor in all cells had a high bone mass secondary to an increase in osteoblast proliferation and bone formation and a subsequent decrease in bone resorption (Elefteriou et al., 2005). It was also supported by a clinical aspect such as the low bone mass of patients affected with reflex sympathetic dystrophy (Schwartzman, 2000).

Several transcription factors have been implicated in mediating this function of the sympathetic tone, and it has long been assumed, although never tested, that this regulation takes place in the osteoblasts (Elefteriou et al., 2005, 2006; Fu et al., 2005). However, because many of these molecular players such as Adrβ2, CREB, and cMyc are by no means osteoblast-specific molecules, there was an urgent need to demonstrate that indeed it is in osteoblasts that this pathway operates. What the experiments presented in this study establish is that it is by acting in the osteoblasts that the sympathetic tone regulates bone mass accrual. It is also through its expression in osteoblasts that CREB regulates osteoblast proliferation downstream of the sympathetic tone. Likewise, it is through its expression in osteoblasts that ATF4 favors *Rankl* expression and osteoclast differentiation downstream of the sympathetic tone. It is noteworthy that these two transcription factors have distinct functions. Indeed, CREB regulates osteoblast proliferation but does not affect osteoclast differentiation, whereas ATF4 affects osteoclast differentiation but is not involved in osteoblast proliferation.

In considering the overall sympathetic mode of regulating bone mass accrual, it is quite remarkable that the sympathetic tone recruits two different transcription factors in the same cell to regulate each arm of bone remodeling. Remarkably, this specificity is conserved when one looks at the main regulator of this function of the sympathetic nervous system, leptin. Indeed, long-term ICV infusion of this hormone in mutant mice lacking, in osteoblasts only, either *Creb* or *Atf4* verified that leptin and the sympathetic tone recruit each of these two transcription factors for different purposes.

Looking more globally at these regulations of bone mass by leptin, it underscores the importance of the various roles played by CREB at several steps in this pathway. Indeed, CREB is mediating serotonin regulation of the sympathetic tone in the ventromedial hypothalamic nuclei, a regulation inhibited by leptin signaling in the brain. Thus, CREB acts upstream of the sympathetic tone (Oury et al., 2010). The present study shows that it also acts downstream of it and in osteoblasts.

This work, by showing that the bulk of the sympathetic regulation of bone mass accrual occurs in osteoblasts, raises the question of its pharmacological relevance. The work of Bonnet et al. (2008) showing that a low dose of β blockers acting through Adrβ2 could prevent gonadectomy-induced bone loss without affecting other function regulated by the sympathetic nervous system is in full agreement with the fact that mice lacking only one allele of *Adrβ2* display high bone mass. As such, it is certainly important if this pathway could be exploited further for the purpose of treating low bone mass disease.

MATERIALS AND METHODS

Animals. *Adrβ2*$_{osb}^{-/-}$, *Creb*$_{osb}^{-/-}$, *Atf4*$_{osb}^{-/-}$, *cMyc-flox/flox*, and *α1(I) Collagen* (2.3-kb *Col1a1* promoter)–*Cre* mice were previously described (de Alboran et al., 2001; Dacquin et al., 2002; Hinoi et al., 2008; Couillard and Trudel, 2009; Yoshizawa et al., 2009). *cMyc-flox/flox* mice were provided by F.W. Alt (Harvard Medical School, Boston, MA) and M. Trudel (Université de Montréal, Montréal, Québec, Canada), and *Creb-flox/flox* mice were provided by G. Schütz (German Cancer Research Center, Heidelberg, Germany). *Adrβ2-flox/flox*, *Creb-flox/flox*, *Atf4-flox/flox*, and *cMyc-flox/flox* littermates were used for the control mice for *Adrβ2*$_{osb}^{-/-}$, *Creb*$_{osb}^{-/-}$, *Atf4*$_{osb}^{-/-}$, and *cMyc*$_{osb}^{-/-}$ mice, respectively. For *Creb*$_{osb}^{+/-}$;*cMyc*$_{osb}^{+/-}$mice analysis, *Creb-flox/+*;*cMyc-flox/+* mice were used as controls. *Creb*$_{osb}^{+/-}$ mice, *Creb-flox/+*, *cMyc*$_{osb}^{+/-}$ mice, and *cMyc-flox/+* mice were independently analyzed. For *Adrβ2*$_{osb}^{-/-}$;*cMyc*$_{osb}^{+/-}$ mice analysis, *Adrβ2-flox/flox*;*cMyc-flox/+* mice were used as control. For *Adrβ2*$_{osb}^{-/-}$ mice, *Adrβ2-flox/flox* mice were used as control. *cMyc*$_{osb}^{+/-}$ mice and *cMyc-flox/+* mice were independently analyzed. Genotyping was performed by PCR analysis of genomic DNA. All mutant mouse strains were on C57BL6/J except *cMyc*$_{osb}^{-/-}$ mice, which are on C57BL6/J and 129Sv/EV. All procedures involving animals were approved by the Columbia University the Institutional Animal Care and Use Committee and conform to the relevant regulatory standards.

Cell culture. Bone marrow–derived osteoblasts were prepared as previously described (Takahashi et al., 1988; Ferron et al., 2010). In brief, mice were sacrificed at the age of 2–3 wk. Bone marrow from tibia was flushed out with PBS, and cells were plated at 0.4 million cells/cm^2 in α-MEM containing 15% FBS. 4 d after plating cells, medium was replaced by α-MEM containing 10% FBS, 5 mM β-glycerophosphate, 100 μg/ml ascorbic acid, and 10 nM dexamethasone and cultured for 7 d. Medium was changed every other day.

Bone histomorphometric analysis. Bone histomorphometry was performed as previously described (Chappard et al., 1987; Parfitt et al., 1987). In brief, lumbar vertebrae were dissected, fixed for 24 h in 10% formalin, dehydrated in graded ethanol series, and embedded in methyl methacrylate resin according to standard protocols. Von Kossa/Von Gieson staining was performed using 7-μm sections for bone volume over tissue volume measurement. BFR was analyzed by the calcein double labeling method. Calcein (Sigma-Aldrich) was dissolved in calcein buffer (0.15 M NaCl and 2% $NaHCO_3$)

and injected twice at 0.125 mg/g body weight on days 1 and 4, and then mice were killed on day 6. 5-µm sections were cleared in xylene and used for BFR measurements. For analysis of the parameters of osteoblasts and osteoclasts, 5-µm sections were stained with toluidine blue and tartrate-resistant acid phosphatase, respectively. Histomorphometric analyses were performed using the OsteoMeasure analysis system (OsteoMetrics).

µCT analysis. Trabecular bone architecture of distal tibia was assessed by using a µCT system (VivaCT 40; SCANCO Medical AG). Tibia bone specimen was stabilized with gauze in a 2-ml centrifuge tube filled with 70% ethanol and fastened in the specimen holder of the µCT scanner. 100 µCT slices, corresponding to a 1.05-mm region distal from the growth plate, were acquired at an isotropic spatial resolution of 10.5 µm. A global thresholding technique was applied to binarize grayscale µCT images in which the minimum between the bone and bone marrow peaks in the voxel gray value histogram was chosen as the threshold value. The trabecular bone compartment was segmented by a semiautomatic contouring method and subjected to a model-independent morphological analysis (Hildebrand et al., 1999) by the standard software provided by the manufacturer of the µCT scanner.

BrdU incorporation. Osteoblast proliferation was assessed in vivo in newborn pups at day 5.5 by injecting thymidine analogue BrdU intraperitoneally. Animals were killed 4 h after BrdU injection. Femora were removed and fixed in 10% formalin at 4°C for 24 h. Bones were demineralized in 25% EDTA at 37°C. Demineralized bones were dehydrated and embedded in paraffin. BrdU labeling was measured in 4-µm sections in the femoral head region using a commercially available kit (Invitrogen). Sections were counterstained with hematoxylin. Proliferating osteoblasts were analyzed using a 40× objective on a microscope (DMLB; Leica) outfitted with a charge-coupled device camera (DXC-S500; Sony) and an OsteoMeasure analysis system.

Biochemistry. Levels of serum CTx were measured using a commercial kit (Immunodiagnostic systems). Western blotting was performed as previously described (Yang et al., 2004; Yoshizawa et al., 2009). In brief, proteins from bone marrow–derived osteoblasts or bones were obtained by homogenizing cells or bones in lysis buffer (25 mM Tris-HCl, pH 7.4, 10 mM Na_3VO_4, 100 mM NaF, 10 mM $Na_4P_2O_7$, 10 mM EGTA, 10 mM EDTA, and 1% NP-40 containing proteinase inhibitor cocktail [Roche]), followed by centrifugation at 14 krpm for 20 min at 4°C. The supernatant was used as extracted proteins. The concentration was measured by Bradford method, and 30 µg of protein was subjected to Western blotting. Anti–phospho-CREB and anti–total CREB antibody were purchased from Cell Signaling Technology. Anti-Adrβ2, anti-cMyc, and anti-ATF4 were purchased from Santa Cruz Biotechnology, Inc.

ICV infusions. Animals were anesthetized with avertin and placed on a stereotaxic instrument (Stoelting). The calvaria was exposed, and a 0.7-mm hole was drilled upon bregma. A 28-gauge cannula (Brain infusion kit II; Alza) was implanted into the third ventricle. The cannula was secured to the skull with cyanoacrylate and attached with Tygon tubing to an osmotic pump (Alza) placed in the dorsal subcutaneous space of the animal. The rate of delivery of leptin (Sigma-Aldrich) was 0.25 µl/h (8 ng/h) for 28 d. In all strains examined, the leptin ICV infusion started at 8 wk of age, and mice were sacrificed at 12 wk of age.

Real-time PCR. Bone marrow–flushed long bones were homogenized in TRIZOL reagent (Invitrogen), and total RNA was extracted according to the manufacturer's instruction. Real-time PCR was performed on DNaseI-treated total RNA converted to cDNA using Taq SYBR green Supermix with ROX (Bio-Rad Laboratories) on an MX3000 instrument (Agilent Technologies); β-*actin* amplification was used as an internal reference for each sample except *Rankl*, for which *Opg* was used for an internal reference.

Statistical analyses. Results are given as means ± SEM. Statistical analyses were performed using unpaired, two-tailed Student's *t* tests.

Online supplemental material. Fig. S1 shows a schematic representation of the peripheral mediation of the leptin-dependent sympathetic regulation of bone mass accrual. Fig. S2 shows gene expression and BrdU incorporation analysis. Fig. S3 shows *Opg* expression in $Adr\beta2_{osb}{}^{-/-}$, $Creb_{osb}{}^{-/-}$, $Atf4_{osb}{}^{-/-}$, and $cMyc_{osb}{}^{-/-}$ mice. Fig. S4 shows bone histomorphometric analysis of $cMyc_{osb}{}^{+/-}$ mice. Online supplemental material is available at http://www.jem.org/cgi/content/full/jem.20102608/DC1.

We thank Dr. Frederick W. Alt and Dr. Marie Trudel for *cMyc-flox/flox* mice and Dr. Günther Schütz for *Creb-flox/flox* mice.

This work was supported by grant DK58883 from the National Institutes of Health (to G. Karsenty).

The authors have no competing financial interests.

Submitted: 15 December 2010
Accepted: 3 March 2011

REFERENCES

Bonnet, N., C.L. Benhamou, L. Malaval, C. Goncalves, L. Vico, V. Eder, C. Pichon, and D. Courteix. 2008. Low dose beta-blocker prevents ovariectomy-induced bone loss in rats without affecting heart functions. *J. Cell. Physiol.* 217:819–827. doi:10.1002/jcp.21564

Chappard, D., S. Palle, C. Alexandre, L. Vico, and G. Riffat. 1987. Bone embedding in pure methyl methacrylate at low temperature preserves enzyme activities. *Acta Histochem.* 81:183–190.

Couillard, M., and M. Trudel. 2009. C-myc as a modulator of renal stem/progenitor cell population. *Dev. Dyn.* 238:405–414. doi:10.1002/dvdy.21841

Dacquin, R., M. Starbuck, T. Schinke, and G. Karsenty. 2002. Mouse alpha1(I)-collagen promoter is the best known promoter to drive efficient Cre recombinase expression in osteoblast. *Dev. Dyn.* 224:245–251. doi:10.1002/dvdy.10100

Datta, N.S., and A.B. Abou-Samra. 2009. PTH and PTHrP signaling in osteoblasts. *Cell. Signal.* 21:1245–1254. doi:10.1016/j.cellsig.2009.02.012

de Alboran, I.M., R.C. O'Hagan, F. Gärtner, B. Malynn, L. Davidson, R. Rickert, K. Rajewsky, R.A. DePinho, and F.W. Alt. 2001. Analysis of C-MYC function in normal cells via conditional gene-targeted mutation. *Immunity*. 14:45–55. doi:10.1016/S1074-7613(01)00088-7

Ducy, P., M. Amling, S. Takeda, M. Priemel, A.F. Schilling, F.T. Beil, J. Shen, C. Vinson, J.M. Rueger, and G. Karsenty. 2000. Leptin inhibits bone formation through a hypothalamic relay: a central control of bone mass. *Cell*. 100:197–207. doi:10.1016/S0092-8674(00)81558-5

Elefteriou, F., S. Takeda, K. Ebihara, J. Magre, N. Patano, C.A. Kim, Y. Ogawa, X. Liu, S.M. Ware, W.J. Craigen, et al. 2004. Serum leptin level is a regulator of bone mass. *Proc. Natl. Acad. Sci. USA*. 101:3258–3263. doi:10.1073/pnas.0308744101

Elefteriou, F., J.D. Ahn, S. Takeda, M. Starbuck, X. Yang, X. Liu, H. Kondo, W.G. Richards, T.W. Bannon, M. Noda, et al. 2005. Leptin regulation of bone resorption by the sympathetic nervous system and CART. *Nature*. 434:514–520. doi:10.1038/nature03398

Elefteriou, F., M.D. Benson, H. Sowa, M. Starbuck, X. Liu, D. Ron, L.F. Parada, and G. Karsenty. 2006. ATF4 mediation of NF1 functions in osteoblast reveals a nutritional basis for congenital skeletal dysplasiae. *Cell Metab.* 4:441–451. doi:10.1016/j.cmet.2006.10.010

Ferron, M., J. Wei, T. Yoshizawa, A. Del Fattore, R.A. DePinho, A. Teti, P. Ducy, and G. Karsenty. 2010. Insulin signaling in osteoblasts integrates bone remodeling and energy metabolism. *Cell*. 142:296–308. doi:10.1016/j.cell.2010.06.003

Fu, L., M.S. Patel, A. Bradley, E.F. Wagner, and G. Karsenty. 2005. The molecular clock mediates leptin-regulated bone formation. *Cell*. 122:803–815. doi:10.1016/j.cell.2005.06.028

Hildebrand, T., A. Laib, R. Müller, J. Dequeker, and P. Rüegsegger. 1999. Direct three-dimensional morphometric analysis of human cancellous bone: microstructural data from spine, femur, iliac crest, and calcaneus. *J. Bone Miner. Res.* 14:1167–1174. doi:10.1359/jbmr.1999.14.7.1167

Hinoi, E., N. Gao, D.Y. Jung, V. Yadav, T. Yoshizawa, M.G. Myers Jr., S.C. Chua Jr., J.K. Kim, K.H. Kaestner, and G. Karsenty. 2008. The sympathetic tone mediates leptin's inhibition of insulin secretion by modulating osteocalcin bioactivity. *J. Cell Biol.* 183:1235–1242. doi:10.1083/jcb.200809113

Karsenty, G. 2006. Convergence between bone and energy homeostases: leptin regulation of bone mass. *Cell Metab.* 4:341–348. doi:10.1016/j.cmet.2006.10.008

Oury, F., V.K. Yadav, Y. Wang, B. Zhou, X.S. Liu, X.E. Guo, L.H. Tecott, G. Schutz, A.R. Means, and G. Karsenty. 2010. CREB mediates brain serotonin regulation of bone mass through its expression in ventromedial hypothalamic neurons. *Genes Dev.* 24:2330–2342. doi:10.1101/gad.1977210

Parfitt, A.M., M.K. Drezner, F.H. Glorieux, J.A. Kanis, H. Malluche, P.J. Meunier, S.M. Ott, and R.R. Recker. 1987. Bone histomorphometry: standardization of nomenclature, symbols, and units. *J. Bone Miner. Res.* 2:595–610. doi:10.1002/jbmr.5650020617

Schwartzman, R.J. 2000. New treatments for reflex sympathetic dystrophy. *N. Engl. J. Med.* 343:654–656. doi:10.1056/NEJM200008313430911

Shi, Y., V.K. Yadav, N. Suda, X.S. Liu, X.E. Guo, M.G. Myers Jr., and G. Karsenty. 2008. Dissociation of the neuronal regulation of bone mass and energy metabolism by leptin in vivo. *Proc. Natl. Acad. Sci. USA.* 105:20529–20533. doi:10.1073/pnas.0808701106

Takahashi, N., T. Akatsu, N. Udagawa, T. Sasaki, A. Yamaguchi, J.M. Moseley, T.J. Martin, and T. Suda. 1988. Osteoblastic cells are involved in osteoclast formation. *Endocrinology.* 123:2600–2602. doi:10.1210/endo-123-5-2600

Takeda, S., F. Elefteriou, R. Levasseur, X. Liu, L. Zhao, K.L. Parker, D. Armstrong, P. Ducy, and G. Karsenty. 2002. Leptin regulates bone formation via the sympathetic nervous system. *Cell.* 111:305–317. doi:10.1016/S0092-8674(02)01049-8

Yadav, V.K., J.H. Ryu, N. Suda, K.F. Tanaka, J.A. Gingrich, G. Schütz, F.H. Glorieux, C.Y. Chiang, J.D. Zajac, K.L. Insogna, et al. 2008. Lrp5 controls bone formation by inhibiting serotonin synthesis in the duodenum. *Cell.* 135:825–837. doi:10.1016/j.cell.2008.09.059

Yadav, V.K., F. Oury, N. Suda, Z.W. Liu, X.B. Gao, C. Confavreux, K.C. Klemenhagen, K.F. Tanaka, J.A. Gingrich, X.E. Guo, et al. 2009. A serotonin-dependent mechanism explains the leptin regulation of bone mass, appetite, and energy expenditure. *Cell.* 138:976–989. doi:10.1016/j.cell.2009.06.051

Yang, X., K. Matsuda, P. Bialek, S. Jacquot, H.C. Masuoka, T. Schinke, L. Li, S. Brancorsini, P. Sassone-Corsi, T.M. Townes, et al. 2004. ATF4 is a substrate of RSK2 and an essential regulator of osteoblast biology; implication for Coffin-Lowry Syndrome. *Cell.* 117:387–398. doi:10.1016/S0092-8674(04)00344-7

Yoshizawa, T., E. Hinoi, D.Y. Jung, D. Kajimura, M. Ferron, J. Seo, J.M. Graff, J.K. Kim, and G. Karsenty. 2009. The transcription factor ATF4 regulates glucose metabolism in mice through its expression in osteoblasts. *J. Clin. Invest.* 119:2807–2817. doi:10.1172/JCI39366